Agar/TiO₂/radish anthocyanin/neem essential oil bionanocomposite bilayer films with improved bioactive capability and electrochemical writing property for banana preservation

Zhikun Yang [a,#], Xiaodong Zhai [a,#], Changcai Zhang [a], Jiyong Shi [a], Xiaowei Huang [a,*], Zhihua Li [a], Xiaobo Zou [a,*], Yunyun Gong [b], Melvin Holmes [b], Megan Povey [b], Jianbo Xiao [c]

[a]Agricultural Product Processing and Storage Lab, School of Food and Biological Engineering, Jiangsu University, Zhenjiang, Jiangsu 212013, China

[b]School of Food Science and Nutrition, University of Leeds, Leeds LS2 9JT, United Kingdom

[c]Institute of Chinese Medical Sciences, State Key Laboratory of Quality Research in Chinese Medicine, University of Macau, Taipa, Macau, China

*Corresponding author. Tel.: +86 511 88780174; Fax: +86 511 88780201; Email: zou_xiaobo@ujs.edu.cn

(Xiaobo Zou)

#These authors contributed equally in this work

*Corresponding author. Tel.: +86 511 88780174; Fax: +86 511 88780201; Email: huangxiaowei@ujs.edu.cn

(Xiaowei Huang)

Abstract

Active agar (AG) bilayer films with bioactive capability and electrochemical writing property were developed for improving the postharvest quality of the banana. The antioxidant and antimicrobial capacity of the films were enhanced with the incorporation of red radish extract (RRE) and neem essential oil (NEO) into AG lower layer. The barrier and mechanical properties, retention of total anthocyanin and NEO content in the bilayer films were effectively improved with addition of TiO₂ into the AG upper layer. Multicolor patterns were successfully written on the bilayer film containing RRE. The AG-TiO₂+AG-RRE-NEO bilayer film exhibited the optimal preservations on banana fruits during the storage period, based on the characterization by fruits appearance, senescent spotting symptom, microbial analysis, weight loss and firmness. Thus, the AG-TiO₂+AG-RRE-NEO bilayer film was expected to be a multifunction packaging material for banana preservation.

Keywords: Active bilayer film; Agar; TiO₂ nanoparticles; Neem essential oil; Red radish anthocyanins;

Introduction

Banana (*Musa nana Lour*) is popular with consumers all over the world due to its rich nutrition and delicious taste (Soradech, Nunthanid, Limmatvapirat, & Luangtana-Anan, 2016). However, bananas are very susceptible to postharvest changes due to their biochemical changes, microbial infections and physiological aging in the supply chain (Lo'Ay & Dawood, 2017).

When it comes to fruit preservation, new bio-based degradable packaging materials are always preferred over conventional packaging materials owing to the extensively acknowledge detrimental effect of the latter on the environment and human health (Zhou, He, Liu, Liao, & Li, 2020). Various bio-based degradable materials have been used to develop fruit packaging films (Jridi, Abdelhedi, Salem, Kechaou, & Menchari, 2020; Rocha, et al., 2018; S. Shankar, Khodaei, & Lacroix, 2021). Among them, agar (AG), a gelatinous polysaccharide extracted from marine red algae, is well-known for its film-forming capacity, has been widely developed as a fruit packaging film (Mostafavi & Zaeim, 2020). To enhance the preservation effect of bio-based degradable packaging films, various active compounds and ingredients have been incorporated into the film to fabricate active film. Especially, some plant extracts have been used as the natural antioxidant to enhance the antioxidant capability of the film (Akhtar, et al., 2013; Aloui, Deshmukh, Khomlaem, & Kim, 2021). The red radish, a traditional anthocyanin-rich edible fruit source (Nariyuki & Kozo, 1963). The red radish extract (RRE) is rich in anthocyanin, which is an ideal natural antioxidant. Hence, the RRE could be added into the film as the antioxidant.

To broad antioxidant film application in fruit preservation, the antimicrobial capability of the film need to be further improved. Essential oils, a generally safe (GRAS) additives by FDA, are of great potential as natural antimicrobials (Turek & Stintzing, 2013). Neem essential oil (NEO) is non-toxic, biodegradable in nature and possess great antimicrobial capability and therefore could be incorporated into the film as an natural antimicrobial agent for improving the antimicrobial capability of the active film (Sani, Geshlaghi, Pirsa, & Asdagh, 2021).

The antimicrobial and antioxidant effects of the active films are related to whether the active ingredients can maintain a certain effective dose for a long time in the film. However, essential oil and plant extract are sensitive to high temperatures, light, and the presence of oxygen (Bakowska, Kucharska, & Oszmianski, 2003; Lfc, et al., 2020). They have been shown to degrade and volatilized rapidly under the influence of these factors so that result in a loss of quality (Turek, et al., 2013).

61 Particularly, UV light irradiation presented the obviously effect on the stability of active compounds

62 embedded into active films in practical application (Turek, et al., 2013). Because the fruit packaging

63 could inevitably be exposed to sunlight during transportation and storage processes. Therefore,

64 improving the UV-blocking property of the active film can effectively prevent the active compounds

65 from degradation and loss, so that the active film has great biological activity during the application

66 time.

67   TiO$_2$ nanoparticles, a generally safe (GRAS) food coloring additives by FDA, are rather cheap and

68 nontoxic, have been widely applied for food preservation due to their UV-absorbing ability and

69 biocompatibility (Ramanavicius & Ramanavicius, 2020; Simonas Ramanavicius, et al., 2020). Hence,

70 TiO$_2$ nanoparticles could be used as an UV-blocking agent for improving the retention of the active

71 compounds embed in the film by protecting the plant extract and essential oil from UV irradiation.

72   Additionally, most labels on food packaging are made of traditional petrochemical feedstock to

73 provide consumers with product information, which can brings significant environmental

74 contamination (Patel, 2015; Yang, Zhai, Zou, Shi, & Xiao, 2020). Therefore, the development of edible

75 label is essential for minimizing food safety risk. Our previous reports confirmed that different color

76 patterns could be printed on the polysaccharide film containing anthocyanins using electrochemical

77 writing (Yang, et al., 2020). However, there are only few reports on printing multicolor patterns on

78 active bilayer film with electrochemical writing.

79   Hence, the aim of this work was to develop active bilayer films with improved bioactive

80 capability and electrochemical writing property for improving the postharvest quality of the banana.

81 The RRE and NEO were incorporated into bottom AG layer as active layer to enhance the bioactive

82 property of the film. The TiO$_2$ nanoparticles were incorporated into upper AG layer as protective layer

83 to improve the retention of the TAC and NEO in the film. Finally, the active bilayer film was used for

84 improving the postharvest quality of banana.

85 **2. Material and methods**

86 **2.1. Materials**

87 Chemical agents including agar, TiO$_2$ nanoparticles, neem essential oil, Folin reagent, ethyl alcohol and

88 2, 2-diphenyl-1-picrylhydrazyl (DPPH) were purchased from Aladdin Industrial Corporation (Shanghai,

89 China) and Sinopharm Chemical Reagent Co., Ltd. (Shanghai, China), respectively.

90 Fresh red radish (cultivar "carmine") and fresh ripen banana samples were brought from local

91 producers (Zhenjiang, China). Banana fruits with uniform size and healthy outer skins were selected.

92 **2.2. Anthocyanins extraction**

93 The extraction method of anthocyanins from red radish was adapted from Yang, et al. (2020). Briefly,

94 the powdered red radish fruit was mixed with ethanol aqueous solution at ratio of 1:60, and then stirred

95 for 30 min. Afterward, the extract solution was passed through the filter paper and freeze-dried to

96 obtain the red radish extract (RRE) powder. The obtained RRE powder was stored at 4 °C in brown

97 air-tight plastic bottle. Total anthocyanins content (TAC) in RRE powder was measured to be 364.0 ±

98 5.8 mg/g by the pH differential method.

99 **2.3. Development of the bilayer film**

100 Agar (AG) solution (3% w/v) was prepared by dissolving AG powder in distilled water at 98 °C with

101 continuously stirring, and glycerol (0.5% w/v) was also added as a plasticizer. The AG-RRE solution

102 was prepared by dissolving a certain amount of RRE powder in the AG solution at 45 °C. The TAC of

103 AG-RRE solution was 6 mg/100 mL. Meanwhile, NEO in ratio of 2.0 g/100 g of AG was dispersed in

104 AG-RRE solution with continuous stirring, and this mixture solution called AG-RRE-NEO solution.

105 Besides, the AG solution only containing a certain amount of NEO (2.0 g NEO/100 g AG) was also

106 prepared, and this mixture solution called AG-NEO. The AG, AG-RRE, AG-NEO and AG-RRE-NEO

107 solution were continuously stirred for 30 min, homogenized at 10000 rpm for 30 min and then degassed

108 with a sonicator for 10 min. Thereafter, AG, AG-RRE, AG-NEO and AG-RRE-NEO solution (6 mL)

109 were poured into a petri dish, respectively. The AG, AG-RRE, AG-NEO and AG-RRE-NEO hydrogels

110 were formed as the lower layer hydrogel when the solution was cooled.

111 In addition, the AG-TiO$_2$ solution was prepared by the addition of TiO$_2$ nanoparticles powders at ratio

112 of 2.0 g/100 g of AG in the AG solution at 45 °C with constant stirring. Subsequently, the mixture was

113 homogenized at 8000 rpm for 5 min, and then degassed at 80 °C for 5 min. Afterward, the AG solution

114 (6 g) was poured over the above-mentioned lower layer hydrogels, respectively. After the AG solution

115 was cooled, AG+AG, AG+AG-RRE, AG+AG-NEO and AG+AG-RRE-NEO bilayer hydrogels were

116 formed. Meantime, 6 g of the AG-TiO$_2$ solution was poured over the AG-RRE-NEO lower layer

117 hydrogel to form the AG-TiO$_2$+AG-RRE-NEO bilayer hydrogel. The above-mentioned bilayer

118 hydrogels were dried at 45 °C to form films and stored at 4 °C with 75% relative humidity (RH) for

119 further use.

120 **2.4. The procedure of electrochemical writing**

The method of printing patterns on the film was adapted from Yang, et al. (2020). Briefly, the bilayer hydrogels incorporating RRE were prepared for electrochemical writing. The electrochemical analyzer (CHI660E, CH Instruments Co., Shanghai, China) was used for printing patterns on the hydrogels. The anode of the electrochemical analyzer made of platinum (Pt) needle (0.5 mm) contacted the upper layer of bilayer hydrogel, and the cathode made of a Pt plate touched the bottom layer surface of the bilayer hydrogel. The movement of the Pt needle was controlled by a DOBOT M1 robotic arm (Yuejiang Technology Co., Ltd., Shenzhen, China) with a step precision of 0.1 μm.

2.5. Characterization of the films

2.5.1. Microstructure observation

Microstructures of cross-section of the prepared films was examined using field emission scanning electron microscopy (FE-SEM) (S-4800, Hitachi High Technologies Corporation, Japan) coupled with energy dispersive X-ray (EDX). The UV–Vis spectrophotometer was used to analyze the optical transmittance of the films in wavelength range of 200–800 nm.

2.5.2. Mechanical test

The mechanic properties (Tensile strength (TS) and elongation-at-break (EB)) of bilayer films were determined with a Tensile Testing Machine (Instron Corporation, Canton, MA) with initial grips separation at 20 mm and tensile speed of 0.6 mm/s. The film thickness was also determined with a hand-held digital micrometer. The sample was cut into a rectangular strip (20 × 20 mm). TS and EB were calculated by the following Eqs. (1) and (2), respectively:

$$TS = \frac{F}{S} \tag{1}$$

$$EB(\%) = \frac{\Delta l}{l_0} \tag{2}$$

Where F is the maximum load; S was the initial cross-sectional area of the films; $\triangle l$ is the extension of the films and l_0 is the initial length of the films.

2.5.3. Water vapor barrier property

The water permeability of the prepared films was determined according to ASTM method (ASTM Standard E96M-05, 1995). A glass cup with silica gel was closed by fixing the prepared bilayer film on top. The cups were placed in a desiccator at 25 °C and 50% RH. The weight of the cups were determined every 4 h until a steady increase in weight was achieved. The water vapor transmission rate (WVTR) and water vapor permeability (WVP) of bilayer films were calculated based on Eqs. (3) and

150   (4):

151     $WVTR = \frac{\Delta m}{A \times \Delta t}$ (3)

152     $WVP = WVTR \times \frac{x}{\Delta p}$ (4)

153   Where $\Delta m / \Delta t$ is the amount of water gain per unit time of transfer; A is the area exposed to water

154   transfer; x is the film thickness, and Δp is the partial pressure difference across the film.

155   2.5.4. Oxygen permeability (OP)

156   The OP of the film was determined referred to the method reported by Akhtar, et al. (2013). The OP

157   value of the film samples were determined by dividing oxygen transmission rate (OTR) by the

158   numerical difference in partial oxygen pressure across the films and multiplying by the average

159   thickness of the film samples, using Eq. (5):

160     $OP = OTR \times \frac{x}{\Delta P}$ (5)

161   Where x is the film thickness and ΔP is the partial pressure of oxygen.

162   2.5.5. Antioxidant capability

163   The antioxidant capability of the bilayer films was evaluated based on the scavenging ability of free

164   DPPH radicals. DPPH assay solution was prepared by mixing 9 mL of the film extract solution with 3

165   mL of methanol solution of DPPH (10^{-3} mol/L). The mixture was incubated in dark at 25 °C for 35 min

166   after shaken for 1 min. The absorbance of the DPPH assay solution was measured at 517 nm. DPPH

167   scavenging activity was calculated by Eq. (6):

168     $DPPH\ scavenging\ activity\ (\%) = \frac{A_{DPPH} - A_S}{A_{DPPH}} \times 100$

169   (6)

170   Where A_{DPPH} is the absorbance value at 517 nm of the methanol solution of DPPH; A_s is the absorbance

171   value at 517 nm of the DPPH assay solution.

172   2.5.6. Antibacterial capability

173   The antibacterial capability of the film against *Escherichia coli* (*E. coli*) and *Staphylococcus aureus* (*S.*

174   *aureus*) was determined referred to agar diffusion method. The film samples were cut into paper disc (6

175   mm diameter) and placed on agar plates containing corresponding bacteria. All the plates were

176   incubated in an incubation chamber at 37 °C for 24 h. The antibacterial capacity of films was evaluated

177   based on the size of the inhibition zones, which was measured with a vernier caliper. All the

178 experiments were performed in triplicate.

2.6. Loss of NEO in bilayer film

180 To simulate the different storage conditions, the loss of NEO in bilayer film under visible light ($\lambda \approx$

181 400–760 nm) and UV light (λ = 320–400 nm with λmax = 350 nm) were measured at 25 °C with 75%

182 RH, respectively. The bilayer film (1.5 g) was mixed with 5 mL deionized water for hydration swelling,

183 then 25 mL hexane was added and continually stirred for 24 h at 25 °C. The mixture containing NEO

184 was centrifuged at 12000 rpm for 10 min. Finally, the UV–Vis spectrophotometer was used to measure

185 the absorbance of the supernatant at 318 nm and 265 nm, respectively. Loss of NEO was calculated

186 based on ratio of decreased amount of NEO in the film with respect to the original amount of NEO in

187 film-forming solution. Triplicate measurements were taken.

2.7. Loss of TAC in bilayer film

189 The loss of TAC in film under UV light ($\lambda \approx$ 400–760 nm) and visible light (λ = 320–400 nm with

190 λmax = 350 nm) was determined follow our previous method with slight modification (Yang, Zou, Li,

191 Huang, & Tahir, 2019). Briefly, the digested film samples (1 mL) were mixed with 0.025 M potassium

192 chloride buffer (pH 1.0) and 0.4 M sodium acetate buffer (pH 4.5), with a dilution factor. The TAC was

193 explicated as pelargonidin-3-glucoside equivalent by measuring the absorbance at 510 nm and 700 nm.

194 TAC was calculated based on Eq. (7).

195 $$TAC = \frac{A \times M_W \times D_f \times 1000}{\varepsilon \times L} \tag{7}$$

196 Where A is $(A_{510} - A_{710})_{PH1.0} - (A_{510} - A_{710})_{PH4.5}$, M_W is the molecular weight of

197 pelargonidin-3-glucoside (433 g/mol), D_f is the dilution factor, ε is the molar absorbance of

198 cyanidin-3-glucoside (26900 M^{-1}cm^{-1}); L is the optical length. The TAC, mg/l was converted to mg/g

199 dry weight of film.

2.8. Application of bilayer films in preserving the banana

201 To investigate preservation effect of the above-mentioned films, fresh banana was immersed in

202 deionized water for 1 h in order to remove any impurities. Afterward, the banana was air-dried at 25 ±

203 1°C and wrapped with the prepared film. The wrapped banana was stored at 25 ± 1°C for 8 days. The

204 postharvest quality of banana at 0, 2, 4, 6, 8 days were recorded.

205 2.8.1. Weight loss and firmness determination

206 The initial weight of banana samples was explicated as W_0. The weight of stored bananas was

207 expressed as W_1. The weight of stored banana was measured at 2, 4, 6 and 8 days. The weight loss was

208 calculated using Eq. (8):

209 $$Weight\ loss\ (\%) = \frac{W_0 - W_1}{W_0} \times 100 \tag{8}$$

210 Firmness of banana was measured using a Texture Analyzer. The tested banana sample was punctured 5

211 mm in depth with a speed of 1.0 mm s^{-1}. The banana firmness was recorded as Newton (N).

212 2.8.2. Assessment of senescent spotting

213 The severity of surface spotting of banana was assessed by the analysis of the number, occurrence and

214 expansion of spotting on banana peel and evaluated by using the scales of 0 to 4. Where score 0 means

215 no dark spot on the peel; score1: 1–25 % dark spot on the peel; score 2 : 26–50 % dark spot on the peel;

216 score 3 : 51–75 % dark spot on the peel; score 4 :76–100 % dark spot on the peel.

217 2.8.3 Microbial analysis

218 Briefly, 20 g of banana samples were milled and transferred to Duran flask with 180 ml of 0.1%

219 peptone water using an aseptic technique. The prepared samples were serially diluted and then spread

220 on potato dextrose agar (PDA) plates. The plates were nurtured at 25 °C for 72 h and total

221 moulds/yeasts colony forming units (CFU) were determined. Triplicate measurements were taken at 0,

222 2, 4, 6 and 8 days of storage.

223 **2.9. Statistical test**

224 Tukey's test was used for the comparisons between the means at the 95% confidence level, the data

225 were analyzed using one-way analysis of variance (ANOVA) in SPSS 15.0 software.

226 **3. Results and discussion**

227 **3.1. Characterization of the films**

228 3.1.1. Morphology analysis

229 The cross section of AG+AG bilayer film was smooth and homogeneous (Fig. 1a), and no clear gap

230 was noticed between the two layers, Indicating that the upper layer and lower layer had outstanding

231 compatibility with each other. With the incorporation of NEO, the cross-section of lower AG layer

232 hardly changed (Fig. 1c). Similar result was also observed by Norcino, Mendes, Natarelli, Manrich,

233 and Mattoso (2020), who found that the cross-section of the pectin film enriched with low

234 concentration of copaiba oil was smooth and compact. When the RRE was incorporated into the AG

235 layer, the AG-RRE layer presented obvious aggregation of spindrift-like structures (Fig. 1b). This result

236 accord with the fact that the presence of hydrophilic compounds in the RRE could lead to some

237 discontinuities in the AG film. However, the AG-RRE layer became less rough (Fig. 1c) with the

238 incorporation of NEO. This change was also similar to those reported by Rocha, et al. (2018). The

239 aggregated TiO_2 nanoparticles with sheet shapes were apparently presented in Fig. 1e, and the result of

240 EDX analysis certified the existence of TiO_2 in the upper AG layer (Fig. S1). The TiO_2 nanoparticles

241 could be observed in the AG-TiO_2+AG-RRE-NEO bilayer film (Fig. 1f). With the addition of TiO_2, the

242 AG layer indicated some irregularities representative of semi-crystalline structures, and the interface of

243 the AG-TiO_2 layer and AG-RRE-NEO layer maintained well-crosslinked. This result revealed that AG

244 based bilayer active films with decent integrity were developed successfully.
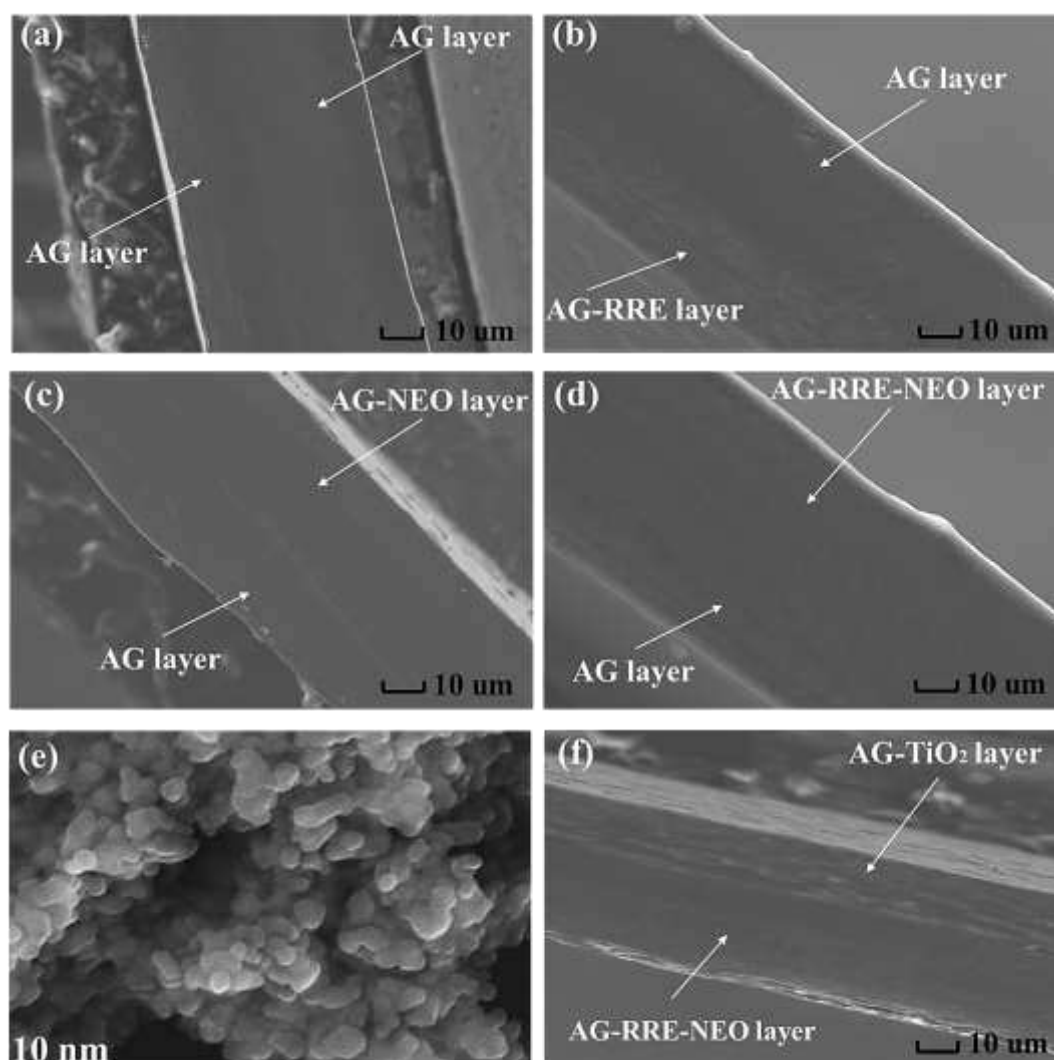
245

246 Figure. 1. SEM images of cross section of AG+AG (a), AG+AG-RRE (b), AG+AG-NEO (c),

247 AG+AG-RRE-NEO (d), TiO_2 nanoparticles (e) and AG-TiO_2+AG-RRE-NEO films (f).

248 3.1.2. Mechanical and Barrier Properties

249   Mechanical properties of bilayer films were shown in Fig.2. The TS of the AG+AG film was

250   obviously decreased with incorporation of the RRE (Fig.2a). This result could be due to the interaction

251   between AG and RRE decreased the strength of the film. The TS of AG+AG film altered little with the

252   incorporation of NEO. This result is in consonance with the micrographs presented above in Fig. 1c,

253   the cross-section of AG layer changed hardly with the incorporation of NEO. Similar trend was also

254   showed in EB of AG based bilayer film (Fig.2b). The EB of AG+AG bilayer film presented a weak

255   change with addition of NEO while the EB of AG+AG film increased significantly with the addition of

256   RRE ($p < 0.05$). This increase in EB could be due to that a large amount of anthocyanin in RRE can

257   increase the mobility of polymeric chain. The TS of AG based bilayer film reached the highest value

258   (30.0 ± 2.9 Mpa) with the incorporation of TiO_2 nanoparticles. This result might be due to the fact that

259   TiO_2 nanoparticles with high surface energy and large specific surface area could facilitate the

260   interfacial bonding between nanoparticles and the AG so that improved the strength of the films (Li &

261   Li, 2010; Liu, et al., 2019). This change was also similar to those observed by Vejdan, Ojagh, Adeli,

262   and Abdollahi (2016), who developed the GN/AG bilayer film incorporated with TiO_2 nanoparticles. In

263   contrast, the EB of the AG based bilayer film decreased significantly ($p < 0.05$) with incorporation of

264   the TiO_2 (Fig.2b). Similar result was also found by Salarbashi, et al. (2016), who conducted that the

265   incorporation of nanoparticles into the polysaccharide matrix limited the moving scale of

266   polysaccharide chain segments, so that decreased the EB of the film.

267   The WVP of the AG+AG film was significantly decreased ($p < 0.05$) to 4.3 ± 0.23

268    $g{\cdot}mm{\cdot}m^{-2}{\cdot}Kpa^{-1}{\cdot}h^{-1}$ after incorporation of RRE (Fig.2c). This because phenolic components in RRE

269   could form noncovalent hydrophobic interactions with AG so that reduce the hydrophilicity of the films.

270   The WVP of the AG+AG film was also significantly decreased with the addition of NEO, because the

271   chemical nature of the NEO exhibited the important effect on improving the water vapor barrier

272   properties of edible films. The WVP of AG+AG-RRE film showed a weak decrease after addition of

273   NEO. Similar result was also observed by Mehdizadeh, Tajik, Langroodi, Molaei, and Mahmoudian

274   (2020), who developed the chitosan-starch film enriched with plant extract and essential oil. The WVP

275   of the AG+AG-RRE-NEO film decreased obviously with the incorporation of TiO_2, indicating that

276   incorporating the nanoparticles into the polymer matrix could increase the flexuous path for water

277   vapor diffusion (Shiv Shankar & Rhim, 2017). This result revealed that the addition of RRE and NEO

278   could decrease the WVP of the bilayer film, and TiO_2 nanoparticles is optimal for improving the water

vapor barrier property of AG bilayer film.

The OP of the AG+AG film, AG+AG-RRE and AG+AG-NEO films were 29.5 ± 2.6, 25.2 ± 1.9 and 25.6 ± 1.7 cm$^3 \cdot \mu m \cdot m^{-2} \cdot d^{-1} \cdot Kpa^{-1}$,respectively (Fig. 2d). This decreased OP of the bilayer film after incorporation of RRE or NEO could be due to that the incorporation of RRE or NEO might decrease the ability of the nonpolar oxygen molecules to condense in the film and decrease the partition coefficient (Wang, Hu, Ma, & Wang, 2016). The OP of the AG-TiO$_2$+AG-RRE-NEO film attained the lowest value (19.5 ± 1.5 cm$^3 \cdot \mu m \cdot m^{-2} \cdot d^{-1} \cdot Kpa^{-1}$), indicating that the incorporation of TiO$_2$ nanoparticle could increase the diffusive path for oxygen molecules (Nafchi, Nassiri, Sheibani, Ariffin, & Karim, 2013; Vaezi, Asadpour, & Sharifi, 2019). This result revealed that the oxygen barrier property of the AG based bilayer film could be improved with the incorporation of RRE and NEO, and it can be
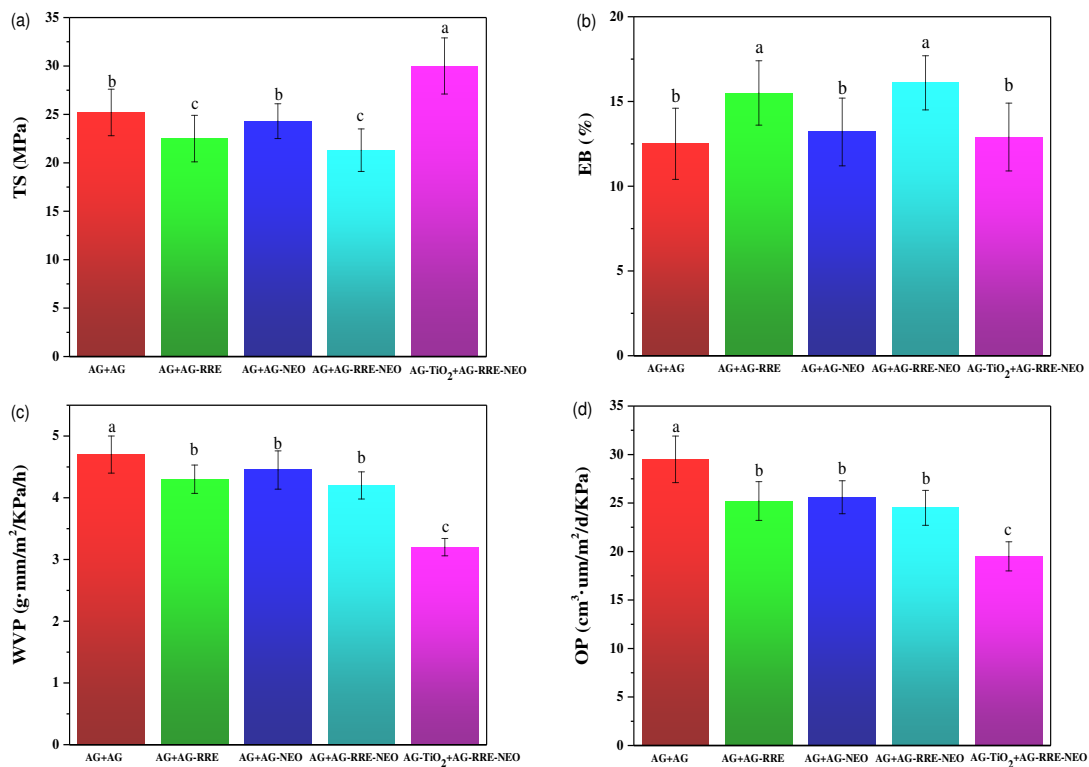
strengthened furtherly by the addition of TiO$_2$.

Figure. 2. TS (a), EB (b), WVP (c), and OP (d) of the AG+AG, AG+AG-RRE, AG+AG-NEO, AG+AG-RRE-NEO, and AG-TiO$_2$+AG-RRE-NEO films.

3.2. The loss of NEO and TAC in the bilayer film

The content of the bioactive compounds in the active film during the storage time is essential for practical application. The loss of NEO and TAC in the films exposed to visible light and UV light were

297 checked in this work, respectively. The loss of NEO in the bilayer film under visible light was shown in

298 Fig. 3a. At the 0 days, the loss of NEO in AG+AG-NEO, AG+AG-RRE-NEO and

299 AG-TiO$_2$+AG-RRE-NEO were 52.4, 53.0% and 48.2%, respectively. This accord with the fact that

300 NEO could suffer a great loss in the drying process (Tian, et al., 2018). In addition, the NEO in

301 AG+AG-NEO, AG+AG-RRE-NEO film were almost absolutely evaporated after 8 days of storage,

302 while the AG-TiO$_2$+AG-RRE-NEO film enhanced its retention time up to 14 days. Similar result was

303 also studied in the loss of NEO in the film under the UV light (Fig. 3b). At the 0 h, the loss percent of

304 NEO in AG+AG-NEO and AG+AG-RRE-NEO film were 43.2% and 42.5%, respectively. After 18 h,

305 the loss of NEO in AG+AG-NEO and AG+AG-RRE-NEO film all increased to 100%. As for

306 AG-TiO$_2$+AG-RRE-NEO film, NEO was completely evaporated or degraded in 28 h. The higher

307 retention of NEO in AG-TiO$_2$+AG-RRE-NEO film under UV light and visible light could be owing to

308 TiO$_2$ nanoparticles with visible light barrier and UV-light absorption property in the upper layer (Fig.

309 S1) that could effectively decrease the evaporation and degradation of NEO in the lower layer.

310 The loss of TAC in the bilayer film under visible light for 32 d was shown in Fig. 3c. After 32 days of

311 storage, the loss of TAC in AG+AG-RRE film and AG+AG-RRE-NEO were 49.9% and 43.6%,

312 respectively. While the loss of TAC in AG-TiO$_2$+AG-RRE-NEO film was 14.8%. This was due to the

313 fact that the incorporating TiO$_2$ nanoparticles into the film can effectively block light (Fig. S1) and

314 oxygen (Fig. 2d) so that protect the anthocyanins from degradation. The loss of TAC in the bilayer film

315 under the UV light was presented in Fig. 3d. The TAC of all bilayer films presented a downward trend

316 during the test time. After 40 h, the TAC of AG+AG-RRE and AG+AG-RRE-NEO film were 3.35 $\pm$

317 0.14 and 3.82 $\pm$ 0.31 mg P3G g^{-1}, respectively. The AG-RRE-NEO film with the incorporation of TiO$_2$

318 maintained the highest TAC (6.76 $\pm$ 0.54 mg P3G g^{-1}). This result can be due to the presence of TiO$_2$

319 nanoparticles with excellent UV absorbing property in the upper layer, which could convert UV light

320 into less detrimental heat or fluorescence. The above-mentioned results proved the validity of TiO$_2$

321 incorporation on maintaining the content of NEO and TAC in AG film during the storage period.

322

323
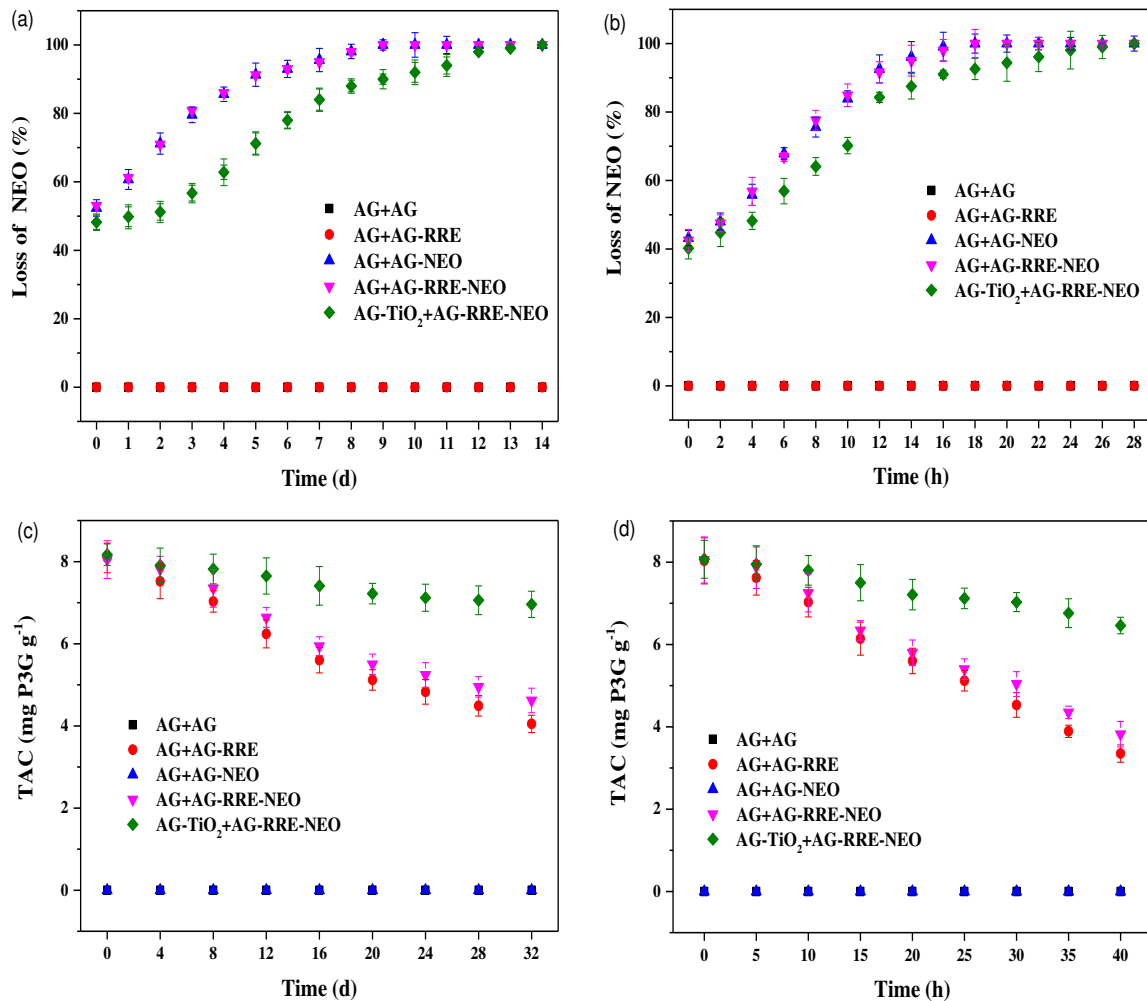
Figure. 3. The loss of NEO in the bilayer films under visible light (a) and UV light (b), and the loss of

TAC in the bilayer films under visible light (c) and UV light (d).

3.3. Antibacterial and antioxidant capability

The photos of inhibition zone of different films were presented in Fig. 4a. The AG+AG bilayer film

showed no inhibition zone for all test bacterial. With the incorporation of RRE, the bilayer film

displayed positive antibacterial effect to all tested bacteria strains, and the diameter of inhibition zone

were 8.7 $\pm$ 0.25 and 7.3 $\pm$ 0.14 mm for *E. coli* and *S. aureus*, respectively. This result could be due

to that the polyphenols in RRE could damage the structure of cell walls and change the permeability of

cell membranes. Notably, the antimicrobial capability of the AG+AG film improved significantly ($p <$

0.05) with the incorporation of NEO, and no significant difference ($p > 0.05$) was studied in

antibacterial activity of AG+AG-NEO and AG+AG-RRE-NEO films. This could be attributed to the

large amount of antimicrobial compounds in NEO (sterols, triterpenoids and active ester derivatives),

which can effectively inhibit microbial growth (Islas, Acosta, G-Buentello, Delgado-Gallegos, & Moreno-Cuevas, 2020). The inhibition zone of bilayer film for *E. coli* and *S. aureus* reached the highest value (24.8 $\pm$ 1.50 and 20.2 $\pm$ 1.10) with the addition of TiO_2. This result may be due to the fact that metal ions can destroy the structure of microbial cells and cause cell inactivation (Khatoon, Rao, Mohan, Ramanaviciene, & Ramanavicius, 2018). Similar result was also found by Khatoon, Nageswara Rao, Mohan, Ramanaviciene, and Ramanavicius (2017).

The antioxidant capability of the AG+AG bilayer film was 4.9 $\pm$ 0.25% (Fig. 4b), and it increased to 13.5 $\pm$ 0.24% with the addition of NEO. The antioxidant capability of the AG bilayer film increased significantly ($p < 0.05$) to 43.9 $\pm$ 1.5% with the incorporation of RRE. Similar result was also reported by Kaya, Ravikumar, Ilk, Mujtaba, and Erkul (2017), who developed the chitosan based edible film enriched with berberis crataegina's fruit extract and seed oil. Our previous study has found that the RRE contained large amount of acylated anthocyanins (Zhai, Li, Zhang, Shi, & Povey, 2018), which showed strong antioxidant capability. This improvement of AG+AG bilayer film could be attributed to the strong antioxidant capability of acylated anthocyanins in RRE. The antioxidant capability of AG+AG-RRE bilayer film presented a weak increase with the addition of NEO and TiO_2, and no significant ($p > 0.05$) difference was observed in antioxidant capability of AG+AG-RRE, AG+AG-RRE-NEO and AG-TiO_2+AG-RRE-NEO films. Similar change was also observed by Lan, Wang, Zhang, Liang, and Zhang (2020), who found that there was no improvement of the antioxidant capability of CS film with the incorporation of TiO_2 nanoparticles. The above-mentioned results illustrated that the antioxidant capability of AG bilayer film was mainly attributed to the incorporation of RRE, and the antibacterial capability of AG bilayer film was mainly due to the addition of NEO and TiO_2. The AG based bilayer film enriched with RRE, NEO and TiO_2 can be used as an effective antimicrobial and antioxidant film.
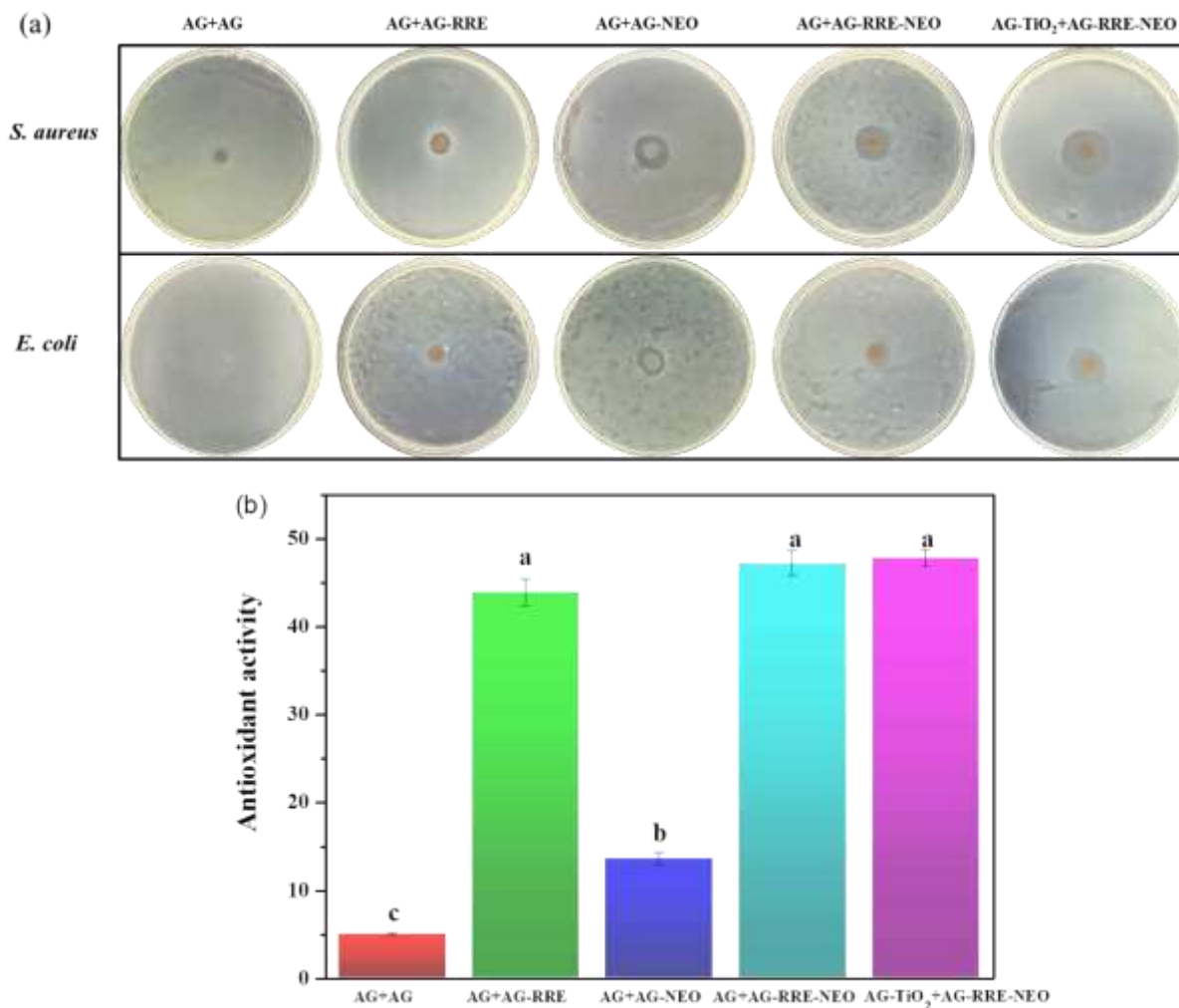
Figure. 4. The antimicrobial capability (a) and antioxidant capability (b) of the AG+AG, AG+AG-RRE, AG+AG-NEO, AG+AG-RRE-NEO, and AG-TiO$_2$+AG-RRE-NEO films.

3.4. The electrochemical writing property of bilayer films

The AG bilayer hydrogels containing high water content were successfully produced in this work. The electrochemical writing pattern with multicolor was developed based on the color changes of anthocyanins induced by hydrogen ions and hydroxyl ions generated from water electrolytic reactions (Yang, et al., 2020). In our previous study, we found that when we use a monolayer hydrogel for electrochemical writing, the entire lower surface of the monolayer hydrogel connected with the Pt plate would be changed to yellow or red due to the water electrolysis reaction (Zhai, et al., 2018). Notably, in this work, all the bilayer hydrogels showed a good performance for electrochemical writing. The English letters (Fig. 5a), smiley face pattern (Fig. 5b) and Chinese characters (Fig. 5c) were successfully written on AG+AG-RRE, AG+AG-RRE-NEO and AG-TiO$_2$+AG-RRE-NEO films, respectively, and no color change was occurred on the surface of the hydrogel connected with the Pt

372 plate. This due to the fact that the water electrolysis reaction round the Pt plate could not change the

373 color of AG or AG-TiO$_2$ layer hydrogel of the bilayer hydrogel without anthocyanins. This result

374 indicated that the AG-RRE layer incorporated with low concentration of NEO will not affected the

375 electrochemical writing property of the bilayer film, and the AG based bilayer film can be used for

376 electrochemical writing with good performance.
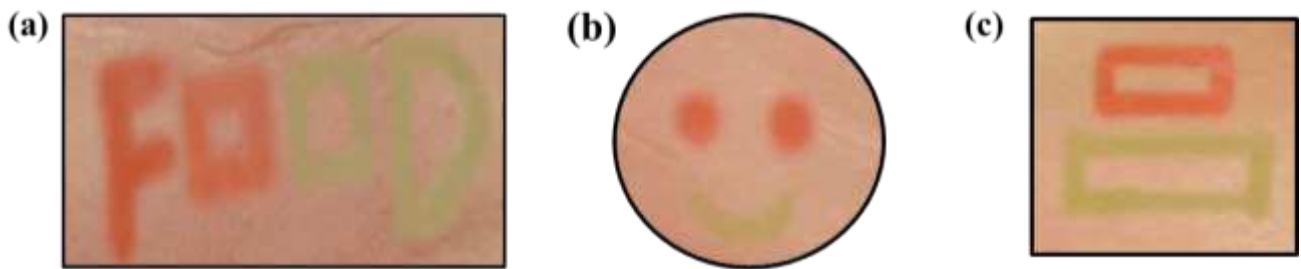
377 Figure. 5. The images of English letters written on the AG+AG-RRE film (a), smiley

378 face pattern written on AG+AG-RRE-NEO (b), and Chinese characters written on

379 AG-TiO$_2$+AG-RRE-NEO film (c).

380 **3.5. Preservation of banana**

381 3.5.1. Appearance and senescent spotting symptom

382 Fig. 6a presented the appearance changes of banana fruits during the storage period. Initially, the

383 surfaces of all bananas were green and intact. After 8 days of storage, the appearance quality of

384 unpackaged bananas was deteriorated obviously, as evidenced by the appearance of black spots and

385 senescent symptom (Fig. 6b). The appearance of black spots in banana peel could be due to the

386 browning reactions and microbial infection (Kamdee, Ketsa, & Doorn, 2009). Compared with the

387 unpackaged banana, the AG+AG packaged banana appeared less black senescent spots (Fig. 6b). This

388 could be due to that the AG based bilayer film can act as a physical barrier to isolate foreign bacteria

389 and reduce the entry of oxygen. As compared with the AG+AG packaged fruit, the bananas packaged

390 with AG bilayer film enriched with functional agent presented a slight change in physical appearance.

391 Notably, AG-TiO$_2$+AG-RRE-NEO bilayer film exhibited the best effect on maintaining the appearance

392 and senescent spotting symptom of banana. This accord with the fact that AG-TiO$_2$+AG-RRE-NEO

393 films maintain the highest content of TAC and NEO (Fig. 3), which would enormously effect the

394 antibacterial and antioxidant capabilities of film during the storage so that could improve the

395 postharvest quality of banana. It was intuitively reflected that the AG based bilayer film incorporated

396 with RRE or NEO can improve the appearance of banana, and the AG-TiO$_2$+AG-RRE-NEO film

397 showed the optimal performance.

398 3.5.2. Microbial analysis

399 The microbial analysis is essential factor for evaluating the preservation effect of banana. The effect of

400 different packaging materials on the total moulds and yeasts counts of the banana samples was shown

401 in Fig. 6c, and all the banana samples presented an upward trend. No significantly difference ($p > 0.05$)

402 was observed in the total moulds and yeasts of each group at the beginning of storage. After 8 days of

403 storage, total moulds/yeasts counts of the unpackaged banana increased to 4.50 ± 0.31 Log CFU/g, and

404 the value of AG+AG, AG+AG-RRE packaged banana were 2.33 ± 0.24, 2.00 ± 0.12, respectively.

405 Notably, the AG based bilayer film incorporated with NEO presented a good performance on inhibiting

406 moulds and yeasts growth, and the AG-TiO$_2$+AG-RRE-NEO film packaged banana showed the lowest

407 moulds and yeasts population (1.33 ± 0.11 Log CFU/g). This effect is consistent with the determination

408 of antimicrobial capacity of the film, indicating that the AG based bilayer film with high antimicrobial

409 activity could effectively inhibited the growth of microbial from the banana. Similar result was also

410 reported by Chowdhury, Teoh, Ong, Rafflisman Zaidi, and Mah (2020), who found that poly(vinyl)

411 alcohol-glyoxal-AuNPs film with enhanced antimicrobial property revealed excellent effect on

412 inhibiting the microbial growth in banana. The comparison of the effect of various packaging materials

413 on microbial analysis of bananas was presented in Table S1. It is noticeable that the bilayer film in

414 present work exhibited the best performance on inhibiting the growth of moulds and yeasts over other

415 reported packaging materials in the literature. This good inhibition effect could be attributed to the

416 presence of TiO$_2$ and NEO in the bilayer film, which are well-known as effective antimicrobial agent.

417 3.5.3. Weight loss and firmness

418 Weight loss is a crucial indicator for evaluating the postharvest quality of fruit. Although all the banana

419 fruits presented an upward trend in weight loss percent (Fig. 6d), the unpackaged fruits presented more

420 rapid in weight loss (13.55%) over packaged fruits during the storage period. The unpackaged fruits

421 were exposed to the environment directly, resulting in rapid water loss. Compared with the AG+AG

422 packaged group, significantly ($P < 0.05$) lower weight loss percent were studied in the AG+AG-RRE,

423 AG+AG-NEO, and AG+AG-RRE-NEO films package fruits (8.92 ± 0.31, 9.03 ± 0.20, and 8.89 ±

424 0.34%, respectively). These results could be due to that bilayer films enriched with functional agents

425 cause a powerful enhancement in the water barrier property so that decreased the loss of water from

426   banana surface. This result was similar to those reported by Zhou, et al. (2020), who observed that

427   films with lower gas penetrability and WVP could improve the quality of stored fruit. Among them, the

428   AG-TiO$_2$+AG-RRE-NEO bilayer film showed the optimal performance on slowing down the weight

429   loss from banana.

430   Fruit firmness is an essential parameter related to the consumer acceptability. Fig. 6e showed that the

431   firmness of all banana fruits decreased during the storage period. After 8 days of storage, the

432   unpackaged banana presented the lowest firmness value (8.5 ± 0.84 N) while the packaged banana

433   exhibited significantly ($P < 0.05$) higher firmness over the unpackaged banana. This slower drop of

434   firmness in the packaged banana could be closely associated with the gas exchange, water loss, and

435   moisture migration, thus, slowing down the softening of the fruit (La, et al., 2021). These results

436   revealed that the AG based bilayer film enriched with RRE, NEO can be utilized to retard the ripening

437   process and slow down the loss of water from banana, and the AG-TiO$_2$+AG-RRE-NEO exhibited the

438   best effect.

439   By comparing the effect of various packaging materials on weight loss and firmness of bananas (Table

440   S2), the packaging materials fabricated in this work presented satisfaction effect among several

441   reported packaging materials in the literature, especially for improving the firmness of banana.

442

443
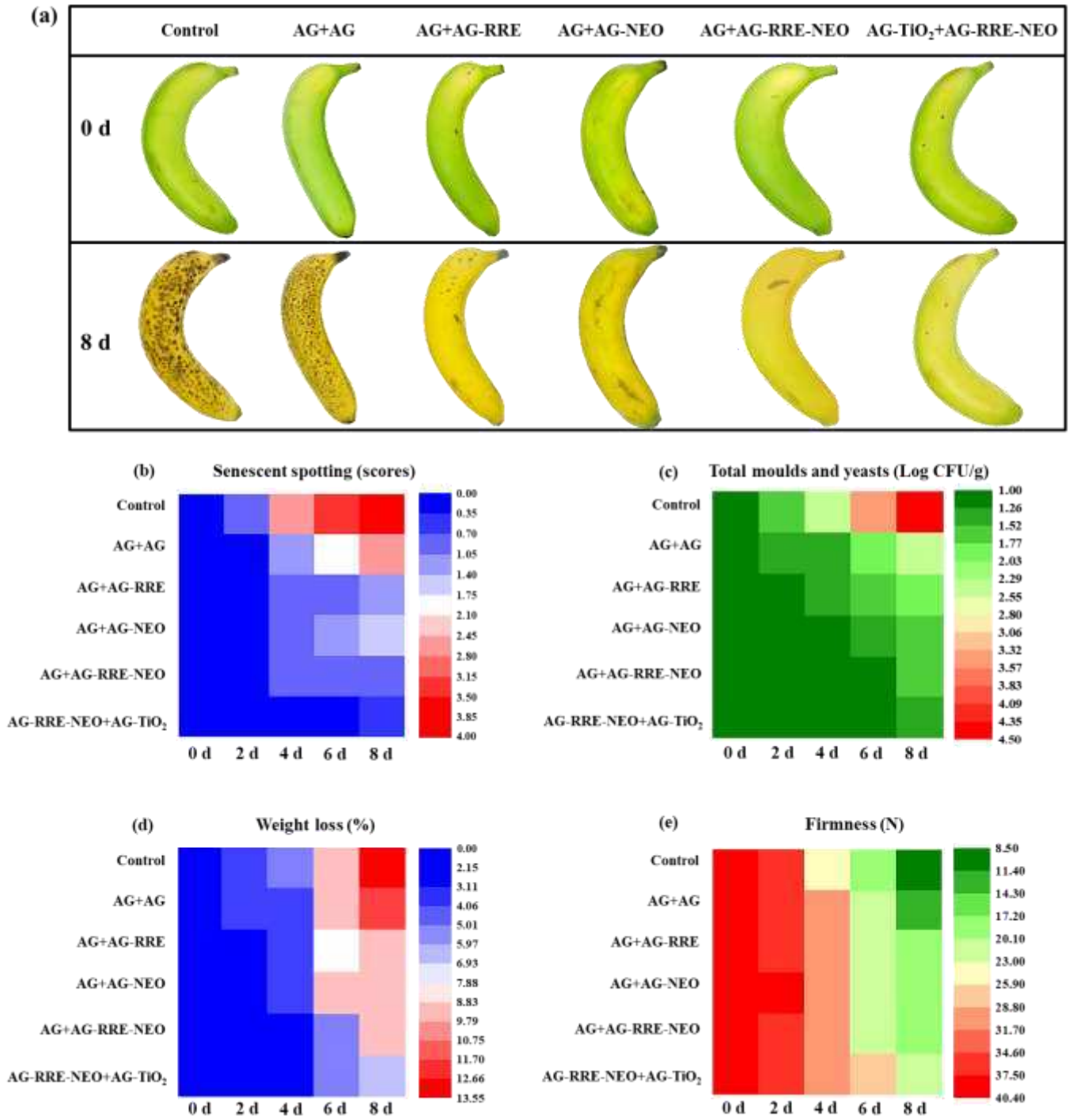
Figure. 6. The bananas preservation indexes of the AG+AG, AG+AG-RRE, AG+AG-NEO,

AG+AG-RRE-NEO, and AG-TiO$_2$+AG-RRE-NEO films during 8 days of storage at room temperature.

A: Physical appearance; b: Senescent spotting; c: Total moulds and yeasts; d: Weight loss; e: Firmness.

447

4. Conclusion

The AG based active bilayer films with enhanced bioactive capability and electrochemical writing property were fabricated successfully for banana preservation. The antioxidant and antimicrobial capacities of the film were improved by the incorporation of RRE and NEO into AG lower layer. The barrier and mechanical properties and the retention of TAC and NEO content in the bilayer film were significantly enhanced by the addition of TiO_2. The multicolor patters were successfully written on the AG based bilayer film. Finally, all the bilayer films were used for preserving the banana. Compared to other films, the AG-TiO$_2$+AG-RRE-NEO bilayer film presented obvious preservations on stored-banana fruits by the analysis of the result of banana appearance, senescent spotting symptom, microbial analysis, weight loss and firmness. Hence, the AG-TiO$_2$+AG-RRE-NEO bilayer film was expected to be a multifunction packaging material for banana preservation.

Supplementary data

Some essential tables and figures to this article.

References

Akhtar, M. J., Jacquot, M., Jamshidian, M., Imran, M., Arab-Tehrany, E., & De Sobry, S. (2013). Fabrication and physicochemical characterization of HPMC films with commercial plant extract: Influence of light and film composition. *Food Hydrocolloids, 31*(2), 420-427.

Aloui, H., Deshmukh, A. R., Khomlaem, C., & Kim, B. S. (2021). Novel composite films based on sodium alginate and gallnut extract with enhanced antioxidant, antimicrobial, barrier and mechanical properties. *Food Hydrocolloids, 113*, 106508.

Bakowska, A., Kucharska, A. Z., & Oszmianski, J. (2003). The effects of heating, UV irradiation, and storage on stability of the anthocyanin–polyphenol copigment complex. *Food Chemistry, 81*(3), 349-355.

Chowdhury, S., Teoh, Y. L., Ong, K. M., Rafflisman Zaidi, N. S., & Mah, S.-K. (2020). Poly(vinyl) alcohol crosslinked composite packaging film containing gold nanoparticles on shelf life extension of banana. *Food Packaging and Shelf Life, 24*, 100463.

Islas, J. F., Acosta, E., G-Buentello, Z., Delgado-Gallegos, J. L., & Moreno-Cuevas, J. E. (2020). An overview of Neem (Azadirachta indica) and its potential impact on health. *Journal of Functional Foods, 74*(104171), 1-13.

Jridi, M., Abdelhedi, O., Salem, A., Kechaou, H., & Menchari, Y. (2020). Physicochemical, antioxidant

and antibacterial properties of fish gelatin-based edible films enriched with orange peel pectin: Wrapping application. *Food Hydrocolloids, 103*, 105688.

Kamdee, C., Ketsa, S., & Doorn, W. (2009). Effect of heat treatment on ripening and early peel spotting in cv. Sucrier banana. *Postharvest Biology & Technology, 52*(3), 288-293.

Kaya, M., Ravikumar, P., Ilk, S., Mujtaba, M., & Erkul, S. K. (2017). Production And Characterization Of Chitosan-Based Edible Films From Berberis Crataegina's Fruit Extract And Seed Oil.

Khatoon, U. T., Nageswara Rao, G. V. S., Mohan, K. M., Ramanaviciene, A., & Ramanavicius, A. (2017). Antibacterial and antifungal activity of silver nanospheres synthesized by tri-sodium citrate assisted chemical approach. *Vacuum, 146*, 259-265.

Khatoon, U. T., Rao, G. V. S. N., Mohan, M. K., Ramanaviciene, A., & Ramanavicius, A. (2018). Comparative study of antifungal activity of silver and gold nanoparticles synthesized by facile chemical approach. *Journal of Environmental Chemical Engineering, 6*(5), 5837-5844.

La, D. D., Nguyen-Tri, P., Le, K. H., Nguyen, P. T. M., Nguyen, M. D.-B., Vo, A. T. K., Nguyen, M. T. H., Chang, S. W., Tran, L. D., Chung, W. J., & Nguyen, D. D. (2021). Effects of antibacterial ZnO nanoparticles on the performance of a chitosan/gum arabic edible coating for post-harvest banana preservation. *Progress in Organic Coatings, 151*, 106057.

Lan, W., Wang, S., Zhang, Z., Liang, X., & Zhang, J. (2020). Development of red apple pomace extract/chitosan-based films reinforced by TiO2 nanoparticles as a multifunctional packaging material. *International Journal of Biological Macromolecules, 168*.

Lfc, A., Qig, A., Mcv, B., Sg, B., Afo, B., Bmh, A., & Sgm, C. (2020). Development of nanoemulsions containing Lavandula dentata or Myristica fragrans essential oils: Influence of temperature and storage period on physical-chemical properties and chemical stability - ScienceDirect. *Industrial Crops and Products*.

Li, S. C., & Li, Y.-N. (2010). Mechanical and antibacterial properties of modified nano-ZnO/high-density polyethylene composite films with a low doped content of nano-ZnO. *Journal of Applied Polymer Science, 116*(5), 2965-2969.

Liu, X., Chen, X., Ren, J., Chang, M., He, B., & Zhang, C. (2019). Effects of nano-ZnO and nano-SiO2 particles on properties of PVA/xylan composite films. *International Journal of Biological Macromolecules, 132*, 978-986.

Lo'Ay, A. A., & Dawood, H. D. (2017). Minimize browning incidence of banana by postharvest active chitosan/PVA Combines with oxalic acid treatment during shelf-life. *Scientia Horticulturae, 226*(226), 208-215.

Mehdizadeh, T., Tajik, H., Langroodi, A. M., Molaei, R., & Mahmoudian, A. (2020). Chitosan-starch film containing pomegranate peel extract and Thymus kotschyanus essential oil can prolong the shelf life of beef. *Meat Science, 163*(May), 108073.108071-108073.108011.

Mostafavi, F. S., & Zaeim, D. (2020). Agar-based edible films for food packaging applications - A review. *International Journal of Biological Macromolecules, 159*, 1165-1176.

Nafchi, A. M., Nassiri, R., Sheibani, S., Ariffin, F., & Karim, A. A. (2013). Preparation and characterization of bionanocomposite films filled with nanorod-rich zinc oxide. *Carbohydrate Polymers, 96*(1), 233-239.

Nariyuki, I., & Kozo, H. (1963). Chromatographic separation and characterization of the component anthocyanins in radish root. *Botanical Magazine Tokyo, 76*(895), 6-13.

Norcino, L., Mendes, J. F., Natarelli, C., Manrich, A., & Mattoso, L. (2020). Pectin films loaded with copaiba oil nanoemulsions for potential use as bio-based active packaging. *Food*

527   *Hydrocolloids, 106*, 105862.

528   Patel, A. K. (2015). Chitosan: Emergence as potent candidate for green adhesive market. *Biochemical*
529   *Engineering Journal, 102*, 74-81.

530   Ramanavicius, S., & Ramanavicius, A. (2020). Insights in the Application of Stoichiometric and
531   Non-Stoichiometric Titanium Oxides for the Design of Sensors for the Determination of
532   Gases and VOCs (TiO2x and TinO2n1 vs. TiO2). *Sensors, 20*(23), 6833.

533   Ramanavicius, S., Tereshchenko, A., Karpicz, R., Ratautaite, V., Bubniene, U., Maneikis, A., Jagminas,
534   A., & Ramanavicius, A. (2020). TiO2-x/TiO2-Structure Based 'Self-Heated' Sensor for the
535   Determination of Some Reducing Gases. *Sensors, 20*(1), 74.

536   Rocha, M., Aleman, A., Romani, V. P., Elvira Lopez-Caballero, M., Carmen Gomez-Guillen, M.,
537   Montero, P., & Prentice, C. (2018). Effects of agar films incorporated with fish protein
538   hydrolysate or clove essential oil on flounder (Paralichthys orbignyanus) fillets shelf-life.
539   *Food Hydrocolloids, 81*(AUG.), 351-363.

540   Salarbashi, D., Mortazavi, S. A., Noghabi, M. S., Fazly Bazzaz, B. S., Sedaghat, N., Ramezani, M., &
541   Shahabi-Ghahfarrokhi, I. (2016). Development of new active packaging film made from a
542   soluble soybean polysaccharide incorporating ZnO nanoparticles. *Carbohydrate Polymers,*
543   *140*, 220-227.

544   Sani, I. K., Geshlaghi, S. P., Pirsa, S., & Asdagh, A. (2021). Composite film based on potato
545   starch/apple peel pectin/ZrO2 nanoparticles/ microencapsulated Zataria multiflora essential oil;
546   investigation of physicochemical properties and use in quail meat packaging. *Food*
547   *Hydrocolloids, 117*, 106719.

548   Shankar, S., Khodaei, D., & Lacroix, M. (2021). Effect of chitosan/essential oils/silver nanoparticles
549   composite films packaging and gamma irradiation on shelf life of strawberries. *Food*
550   *Hydrocolloids*.

551   Shankar, S., & Rhim, J.-W. (2017). Preparation and characterization of agar/lignin/silver nanoparticles
552   composite films with ultraviolet light barrier and antibacterial properties. *Food Hydrocolloids,*
553   *71*, 76-84.

554   Soradech, S., Nunthanid, J., Limmatvapirat, S., & Luangtana-Anan, M. (2016). Utilization of shellac
555   and gelatin composite film for coating to extend the shelf life of banana. *Food Control*,
556   S0956713516306089.

557   Tian, X., Gao, C., Yang, Y., Shen, X., Huang, M., Liu, S., & Tang, X. (2018). Retention and release
558   properties of cinnamon essential oil in antimicrobial films based on chitosan and gum arabic.
559   *Food Hydrocolloids, 84*, 84-92.

560   Turek, C., & Stintzing, F. C. (2013). Stability of Essential Oils: A Review. *Comprehensive Reviews in*
561   *Food Science and Food Safety, 12*(1), 40-53.

562   Vaezi, K., Asadpour, G., & Sharifi, H. (2019). Effect of ZnO nanoparticles on the mechanical, barrier
563   and optical properties of thermoplastic cationic starch/montmorillonite biodegradable films.
564   *International Journal of Biological Macromolecules, 124*, 519-529.

565   Vejdan, A., Ojagh, S. M., Adeli, A., & Abdollahi, M. (2016). Effect of TiO2 nanoparticles on the
566   physico-mechanical and ultraviolet light barrier properties of fish gelatin/agar bilayer film.
567   *LWT - Food Science and Technology, 71*, 88-95.

568   Wang, H., Hu, D., Ma, Q., & Wang, L. (2016). Physical and antioxidant properties of flexible soy
569   protein isolate films by incorporating chestnut (Castanea mollissima) bur extracts. *LWT - Food*
570   *Science and Technology, 71*, 33-39.

571   Yang, Z., Zhai, X., Zou, X., Shi, J., & Xiao, J. (2020). Bilayer pH-sensitive colorimetric films with
572   light-blocking ability and electrochemical writing property: Application in monitoring crucian
573   spoilage in smart packaging. *Food Chemistry, 336*, 127634.

574   Yang, Z., Zou, X., Li, Z., Huang, X., & Tahir, H. E. (2019). Improved Postharvest Quality of Cold
575   Stored Blueberry by Edible Coating Based on Composite Gum Arabic/Roselle Extract. *Food
576   and Bioprocess Technology, 12*(1).

577   Zhai, X., Li, Z., Zhang, J., Shi, J., & Povey, M. (2018). Natural Biomaterial-Based Edible and
578   pH-Sensitive Films Combined with Electrochemical Writing for Intelligent Food Packaging.
579   *Journal of Agricultural and Food Chemistry, 66*(48).

580   Zhou, W., He, Y., Liu, F., Liao, L., & Li, J. (2020). Carboxymethyl chitosan-pullulan edible films
581   enriched with galangal essential oil: Characterization and application in mango preservation.
582   *Carbohydrate Polymers, 256*(3), 117579.

583